

Effect of Temperature on the Tensile Mechanical Properties and Creep Performance of Wood-plastic Composites

Fei Xi  ^{a,*} Jun Yang, ^{a,*} Longlong Zhao  ^b and Yang Wei ^b

Uniaxial tensile tests of recycled waste wood plastic composites were conducted at 20, 40, and 60 °C. High density polyethylene (HDPE, 30%) was reinforced with poplar wood (50%), and calcium carbonate (15%), with 5% additives. The load values for three stress levels of 15%, 30%, and 45% were determined at each temperature. Subsequently, 24-h short-term creep tests of WPC were conducted under nine operating conditions. Both the ultimate strength and elastic modulus of the material was found to decrease with increasing temperature. The modulus and ultimate strength decreased from 3890 and 15.0 MPa at 20 °C to 1970 and 7.1 MPa at 60 °C, respectively. Furthermore, the stress-strain curves of WPC specimens exhibit plastic behavior when the temperature exceeded 40 °C. The creep deformation of WPC was positively correlated with temperature and stress level. The Findley model exhibited distortion in fitting the creep performance of WPC only under the condition of 60 °C and 15% stress level. Conversely, the fractional-order model demonstrated a better fitting effect on the steady-state creep characteristics of WPC under this working condition.

DOI: 10.15376/biores.21.1.1824-1835

Keywords: WPC mechanical properties; Fractional order model; HDPE; Poplar wood; Findley model

Contact information: a: College of Art & Designing, Nanjing University of Finance and Economics, Nanjing 210023, China; b: College of Civil Engineering, Nanjing Forestry University, Nanjing 210037, China;

* Corresponding author: 9120181067@nufe.edu.cn, 9120061028@nufe.edu.cn

INTRODUCTION

Wood plastic composites (WPCs) are materials composed of wood fibers, wood powder, or wood cellulose, and plastic resins such as polyethylene (PE), polypropylene (PP), or polyvinyl chloride (PVC); they are often manufactured through various extrusion processes (Zhao *et al.* 2021; Elsheikh *et al.* 2022). They possess advantages such as good wood-like properties, strong weather resistance, excellent resistance to decay, high plasticity, and environmental friendliness (Xi and Zhao 2022). The sample production process of WPC is prepared by a two-step extrusion molding process after mixing polyolefin, wood powder, and additives. The particles often are placed in an extruder for extrusion molding after using a parallel twin-screw extruder for granulation (Golmakani *et al.* 2021; Golmakani *et al.* 2021; Xi and Zhao 2022). Creep is the gradual plastic deformation of materials under sustained stress, typically occurring under constant stress or continuous loading conditions. This plastic deformation increases gradually over time, and there may be fracture of the material. Creep phenomena are significant in material engineering and structural design, especially due to creep characteristics of the wood-based composites. The failure mode, the bearing capacity, the stiffness, and the deformation of

its components can be expected to be impacted by long-term loading (Ratanawilai and Srivabut 2021).

When using WPCs under different external conditions, such as temperature changes, their performance variations are difficult to predict (Pulngern *et al.* 2016; Van *et al.* 2019). Feng and Zhao (2022) analyzed the influences of molding temperature, pelleting temperature, coupling agent screw speed, and other technological factors on the creep properties of WPC under different loads. Chang *et al.* (2018) studied the effects of temperature-induced strain on creep behavior of wood-plastic composites, indicating that the creep test under an ambient environment could successfully simulate long-term creep with increasing temperatures. Alrubaie *et al.* (2020a) conducted a comparative study on the flexural creep behavior of wood-plastic composites (WPCs) prepared from thermally modified wood and high-density polyethylene (HDPE) panels, finding that the addition of thermally modified wood improved the creep resistance of WPCs. Wiczenbach *et al.* explored the effect of wood powder and nanoclay particle content on composites mechanical behavior made with polyethylene matrix. Dai *et al.* (2022) confirmed that the incorporation of GFRP significantly enhances the flexural strength and creep resistance of WPCs, offering a reinforcement strategy for producing high-performance WPCs.

Zhao and Xi and their co-authors established a short-term creep model for WPCs through experimental data fitting, providing a basis for deformation control in short-term service scenarios (Zhao *et al.* 2021; Xi *et al.* 2023). Zhang *et al.* (2024) developed a multivariable-coupled short-term creep model by incorporating different stress levels and temperature conditions. Alrubaie *et al.* (2020b,c) systematically investigated the creep strain patterns under hygrothermal environments through experiments and modeling, establishing a predictive model for hygrothermal creep behavior. They further extended the research to practical structural applications, enabling a cross-scale study from material properties to structural behavior, which provides theoretical support for its promotion in large-span lightweight structures (Alrubaie *et al.* 2020d).

Models for fitting the creep characteristics of WPC materials mainly include the Kelvin-Voigt model (Zong *et al.* 2020), Findley power law model (Zhang *et al.* 2024), Burgers model (Fu *et al.* 2020), *etc.* In this study, WPCs were fabricated using a two-step extrusion molding process (Zhao *et al.* 2025). Short-term creep tests were conducted under different temperature conditions and stress levels for 24 h. A computational model describing the short-term creep behavior of the material was established, providing a theoretical basis and experimental evidence for the engineering application of materials under different temperature conditions.

EXPERIMENTAL

Material

The WPC used in this study consisted of 30% polyolefin (HDPE), 50% poplar wood powder, 15% calcium carbonate, and 5% additives. Tensile performance tests of WPC were conducted under temperature conditions of 20, 40, and 60 °C, following ASTM D-143 (2014). Three parallel specimens were tested for each group, with specimen numbers ranging from 1 to 3. As shown in Fig. 1, the material testing was conducted on a 50 kN high and low temperature universal creep testing machine with the model number UTM5504GD. A gauge extensometer with the model number EAG-050M-0100-L was positioned in the central region of the specimen, with a gauge length of 50 mm and a range

of 10%. The test was conducted under beam displacement control, with a loading rate of 0.5 mm/min. Load and deformation data were recorded by the computer for the analysis of the mechanical properties of the material under various temperature conditions. The test results indicate the ultimate tensile load of WPC under each temperature condition, measured in N. Table 1 shows that the maximum coefficient of variation of the tensile ultimate load of WPC was only 10.9%, indicating that the WPC was a material with good mechanical stability and did not exhibit increased discreteness with increasing temperature.

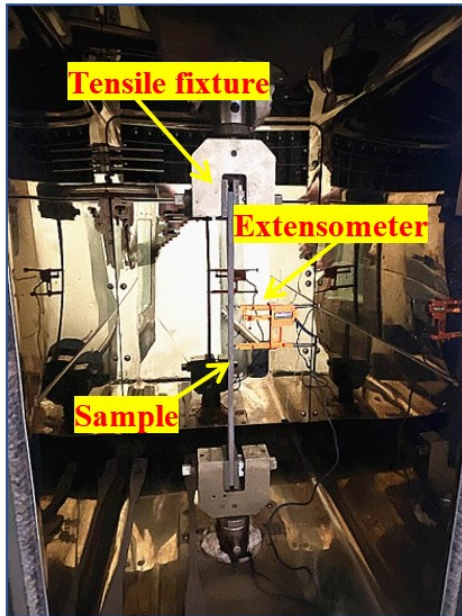


Fig. 1. Experimental schematic diagram

Table 1. Tensile Test Results (N)

	20 °C	40 °C	60 °C
1	639.9	584.3	380.1
2	834.6	669.1	353.2
3	781.3	552.9	327.1
AVE	751.9	602.1	353.5
SD	82.2	49.1	21.6
CoV/%	10.9	8.5	6.1

Note: AVE means average value, SD is standard deviation; CoV represents coefficient of variation

Stress-Strain Relationship

The typical stress-strain relationship of WPC under different temperature conditions is depicted in Fig. 2. At a temperature of 20 °C, the curve exhibited linear elastic behavior, with an elastic modulus of 3890 MPa and an ultimate strength of 15.0 MPa. As the temperature rose to 40 °C, the ultimate strength decreased by 19.9% to 12.0 MPa, and the elastic modulus decreased by only 13.7% to 3360 MPa. At this point, the WPC specimen exhibited plastic deformation characteristics, and the stress-strain relationship showed significant nonlinearity in the later stages. As the temperature continued to increase, both the elastic modulus and ultimate strength of WPC steadily decreased. The ultimate strength decreased to 7.1 MPa, and the elastic modulus decreased to 1970 MPa, representing only 47.0% and 50.6% of their values at 20°C, respectively, and 58.7% and 58.6% of their values at 40 °C, respectively.

At a temperature of 20 °C, the stress-strain curve of the WPC specimen exhibited linear behavior, indicating a linear elastic relationship. Therefore, it can be analyzed using a linear elastic model,

$$\sigma = E\epsilon \quad 0 < \epsilon \leq \epsilon_u \quad (1)$$

where σ represents the tensile stress when the strain is ϵ , and when $\epsilon = \epsilon_u$, $\sigma = \sigma_{tu}$.

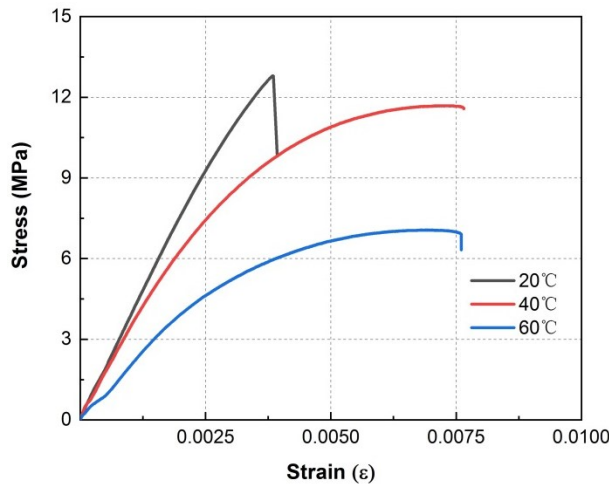


Fig. 2. Stress-strain relationship

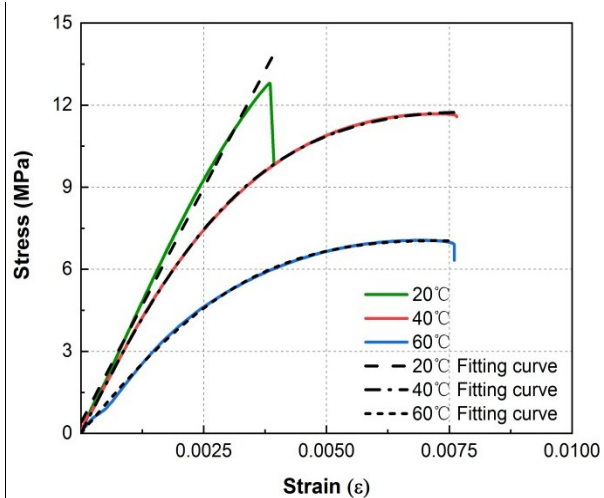


Fig. 3. Fitting results

As the temperature was increased, the stress-strain relationship of WPC exhibited significant plastic characteristics. This study attempted to describe the stress-strain relationship of WPC at 40 °C and 60 °C using the Popovics modified model. The calculation formula of the Popovics model (Wu and Wei 2015) is shown in Eq. 2, where $x = \epsilon / \epsilon_y$, and σ_y and ϵ_y represent the stress and strain corresponding to the yield point, respectively.

$$f(x) = \frac{\sigma}{\sigma_y} = \frac{x \cdot a}{a - 1 + x^a} \quad (2)$$

The fitting results of the stress-strain relationship of WPC under different temperature conditions are depicted in Fig. 3. All fits of the curves exhibited regression coefficients greater than 0.99, indicating that the Popovics modified model can effectively predict the mechanical properties of WPC under high temperature conditions.

Creep Test

The creep performance of WPC samples under different temperature conditions was tested using the standard test method ASTM D3130-11 (2019). Three stress levels of 15%, 30%, and 45% were set for each temperature group, with the corresponding load values determined based on the material testing results, as shown in Table 2.

Table 2. Creep Load Capacity Values (N)

Stress Levels	20 °C	40 °C	60 °C
15%	110	80	50
30%	220	160	100
45%	330	240	150

The 24-h tensile creep tests of WPC under different temperature conditions were conducted on a high and low-temperature creep testing machine with model number UTM5504-GD and a load capacity of 50 kN. The temperature of the specimens was controlled using a high and low-temperature environmental chamber with model number WGDY-7350L. Due to the expansion and contraction of specimens during temperature ramp-up, ramp-down, and temperature holding processes, the specimens were equilibrated in the environmental chamber for 30 min to ensure that the specimen temperature reached the test temperature before loading. During loading, beam displacement control was employed, with a loading speed of 1 mm/min. The holding load commenced when the load reached the specified stress level and was maintained for 24 h. The test was terminated upon specimen failure. The computer recorded the applied load and displacement every minute to analyze the creep behavior of the material under different temperature and stress level conditions.

RESULTS AND DISCUSSION

The curves showing the deformation of WPC under different temperature and stress level conditions over a 24-h holding period are illustrated in Fig. 4. The primary factor affecting the creep rate of WPC was the stress level. When the temperature remained constant, specimens subjected to a stress level of 15% underwent a short period of primary creep, followed by sustained or even decreasing deformation. Specimens subjected to a stress level of 30% quickly transitioned to secondary creep after the primary creep stage, during which the deformation rate remained relatively stable and exhibits a more linear relationship. At a stress level of 45%, the creep process of the specimens was similar to that at 30%, but the slope of the curve during the secondary creep stage increased significantly. When the stress level remained constant, the creep behavior of the specimens under different temperature conditions was generally consistent.

The results of the creep tests are presented in Table 3. In the table, d_1 represents the initial deformation of the specimens when the load reaches the stress level, while d_2 represents the final deformation of the specimens after 24 h of holding. Δd indicates the creep deformation of the specimens over 24 h, and λ represents the ratio of creep deformation to initial deformation. It can be concluded that at stress levels of 15% and 30%, the creep increased continuously with rising temperature, conforming to the Arrhenius law dominated by thermally activated viscous flow. At the 45% stress level, however, creep exhibited a non-monotonic trend as temperature rose. This occurs because the high temperature of 60 °C caused the polymer matrix to be in a highly active state, which critically coupled with the high stress of 45%. The resulting extremely high thermo-mechanical driving potential caused the molecular chain network to undergo rapid rearrangement and orientation analogous to macroscopic “yielding” well before the 24-hour mark, thereby dissipating the viscoplastic potential energy that would otherwise be released over longer term creep. This rapid adjustment led to a very large proportion of instantaneous plastic deformation (d_1) during the initial loading stage. Subsequently, the material entered a new quasi-stable mechanical state defined by a stabilized damage network and failed interfaces. In this state, both the driving force and the pathways for further deformation were significantly reduced. As a result, within the 24-hour observation window, the additional creep increment became smaller.

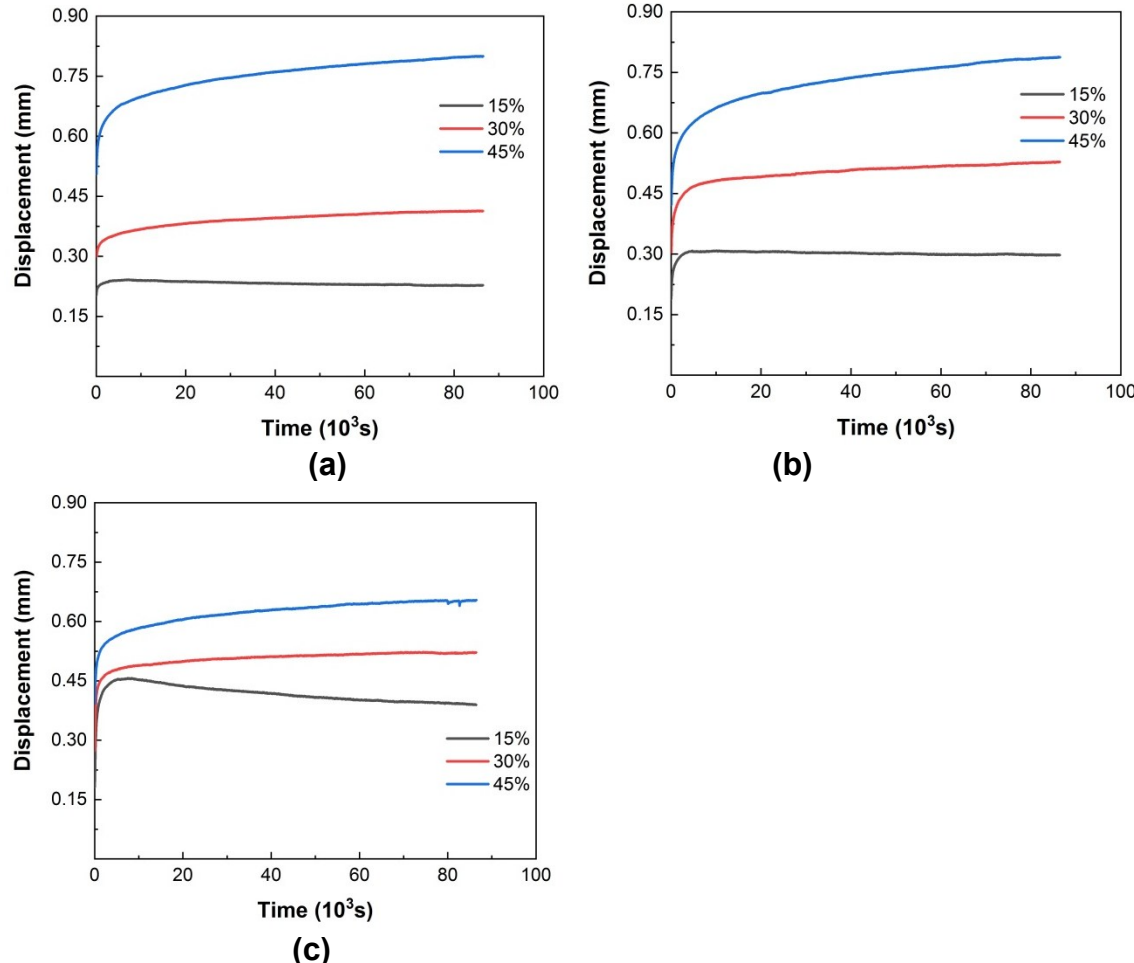


Fig. 4. Short term creep curve: (a) 20 °C, (b) 40 °C, (c) 60 °C

Table 3. Creep Test Results

Temperature	Stress level	d_1 (mm)	d_2 (mm)	Δd (mm)	λ (%)
20	15%	0.2	0.2	0.03	12.5
	30%	0.3	0.4	0.1	46.4
	45%	0.5	0.8	0.3	58.3
40	15%	0.2	0.3	0.1	57.6
	30%	0.3	0.5	0.2	73.6
	45%	0.4	0.8	0.4	86.3
60	15%	0.2	0.4	0.2	114.8
	30%	0.3	0.5	0.3	90.5
	45%	0.4	0.7	0.3	66.7

The histogram of creep deformation for each specimen is illustrated in Fig. 5. When the stress levels were 15% and 30%, the creep deformation increased continuously with temperature. However, when the stress level was 45%, the creep deformation initially increased and then decreased with increasing temperature. When the temperature remained constant, the creep deformation increased with increasing stress level.

At a temperature of 20 °C, the creep deformation of WPC at a stress level of 30% was 3.7 times that at 15%, and at 45%, it was 1.9 times that at 30%. When the temperature rose to 40 °C, the multiples compared to 15% and 30% were 1.8 and 1.1, respectively.

When the temperature reached 60°C, these multiples decreased to 1.2 and 0.7, respectively. This indicates that at higher temperatures, the influence of stress level on the creep deformation of WPC decreased.

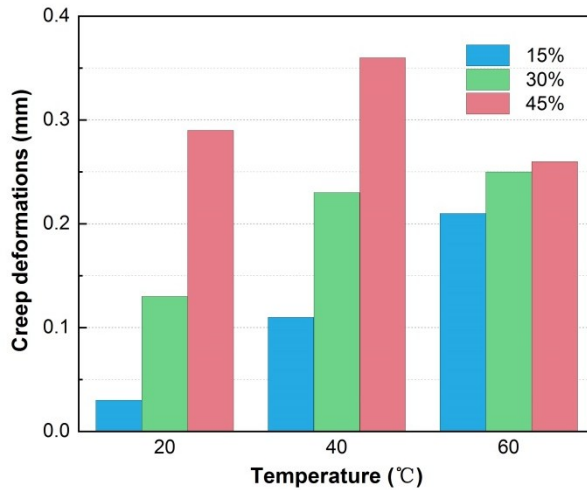


Fig. 5. Statistics of creep variables

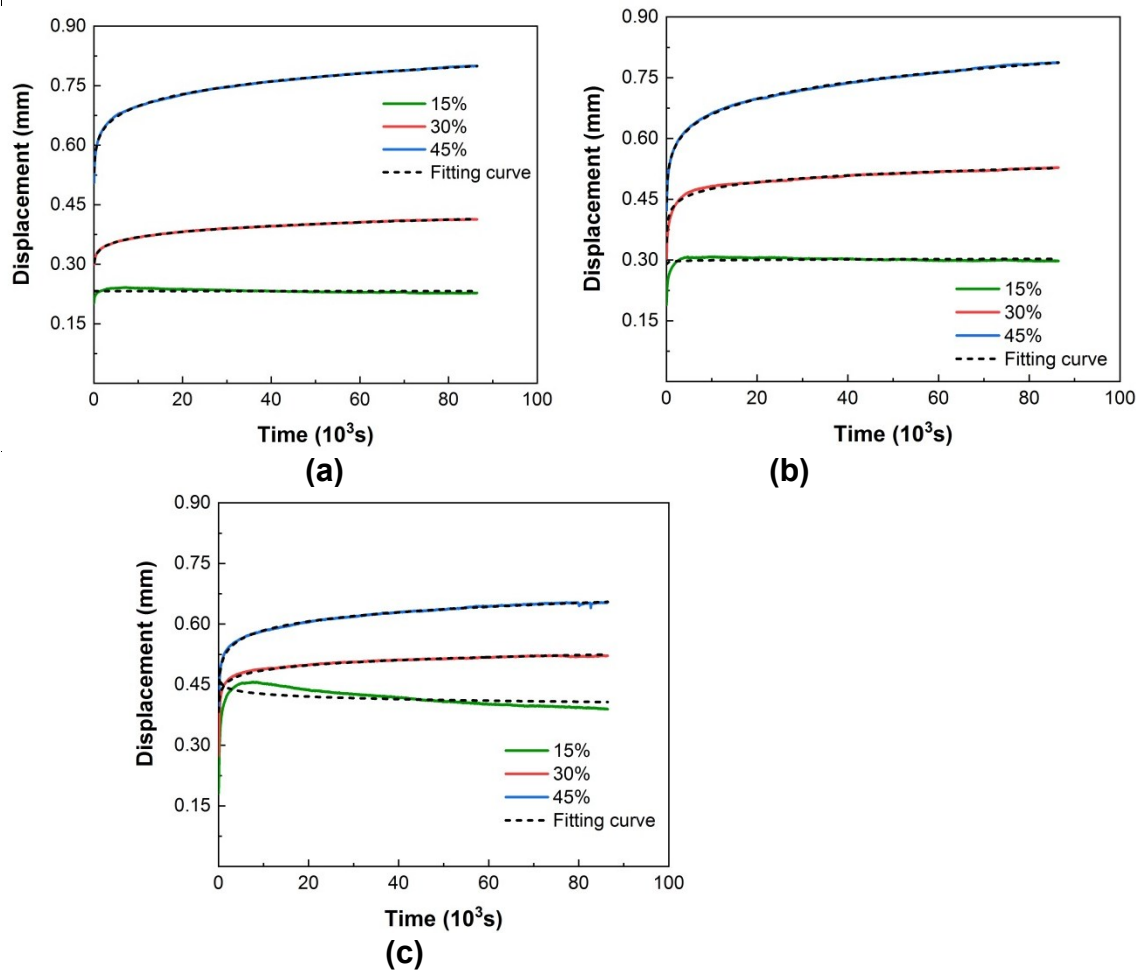


Fig. 6. Findley model fitting results: (a) 20 °C, (b) 40 °C, (c) 60 °C

Findley Model

The Burgers model provides a good fit for the material properties of WPC after entering steady-state creep at room temperature, but it almost fails to predict transient creep (Zhao *et al.* 2022). In contrast, the Findley model exhibits high accuracy in fitting the results of tensile and compressive creep tests of WPC at various stress levels. Proposed in 1944, the Findley model can effectively predict the creep behavior of polymer composites (Liu *et al.* 2013). The formula is given by Eq. 3,

$$\varepsilon(t) = \varepsilon_0 + at^b \quad 0 \leq t \leq 86400s \quad (3)$$

where ε_0 represents the initial strain, while a and b are material constants.

The fitting results of the short-term creep for each specimen using the Findley model are shown in Fig. 6. When the temperature was constant, the goodness of fitting results increased with the increase in stress level. At 60 °C, the regression coefficients for the three stress levels of 15%, 30%, and 45% were 0.17, 0.94, and 0.99, respectively. However, when the stress level was constant, the fitting effect decreased with increasing temperature. For example, at a stress level of 30%, the coefficient of determination (R^2) was 0.99 at 20 °C, it decreased to 0.97 at 40 °C, and for WPC tested at 60 °C, the regression coefficient of the Findley model for short-term creep was 0.94. As depicted in Fig. 6c, it can be observed that the Findley model exhibited significant distortion in fitting the creep performance of specimens tested under the condition of 60 °C and 15% stress level.

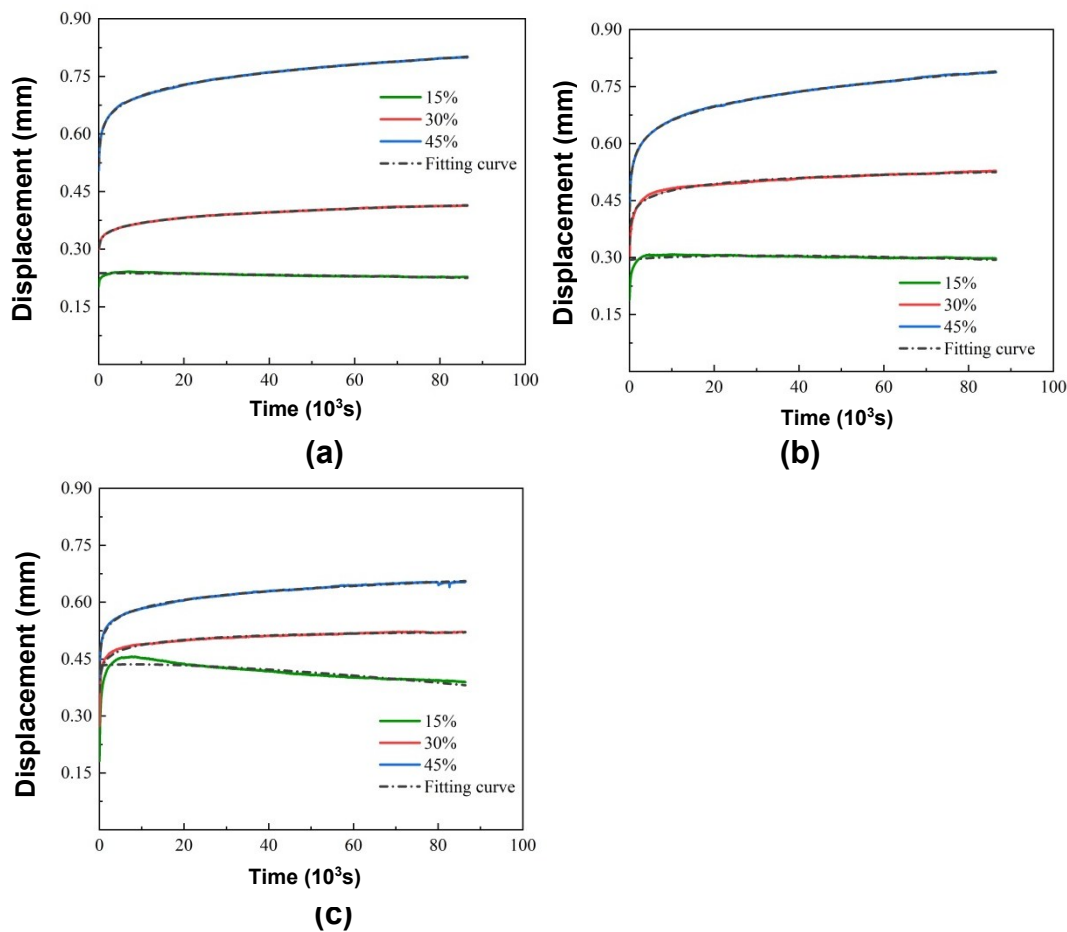


Fig. 7. Fractional order model fitting results: (a) 20 °C, (b) 40 °C, (c) 60 °C

Fractional Order Model

Heymans *et al.* (1994) utilized fractional calculus to represent the stress-strain relationship of viscoelastic materials lying between purely elastic and purely viscous bodies, employing fractional order viscoelastic elements to replace the Kelvin units in the Burgers model and thus deriving a new fractional order viscoelastic model. The equation is represented as follows, where Γ denotes the gamma function:

$$\varepsilon(t) = \frac{\sigma}{E_1} + \frac{\sigma_a}{\eta_a} \frac{t^\alpha}{\Gamma(1+\alpha)} + \frac{\sigma}{\eta_1} t \quad 0 \leq \alpha \leq 1 \quad 0 \leq t \leq 86400s \quad (4)$$

The prediction results of creep behavior of WPC using the fractional order model are illustrated in Fig. 7. At temperatures of 20 and 40 °C, the goodness of fit for stress levels of 30% and 45% was 0.99. When the temperature was 60 °C, the goodness of fit for a stress level of 30% was 0.97, which increased to 0.99 for a stress level of 45%. At a stress level of 15%, the fractional order model exhibits a good fit for the steady-state creep stage of WPC under various temperature conditions. The regression coefficients were significantly higher compared to the Findley model, but they did not reach 0.9.

CONCLUSIONS

1. The tensile strength and modulus of elasticity of wood-polymer composites (WPCs) formed from high density polyethylene (30%), poplar wood (50%), calcium carbonate particles (25%) and additives (5%) decreased with increasing temperature. When the temperature reached 40 °C, the ultimate strength and modulus of elasticity decreased by 19.9% and 13.7%, respectively, compared to 20 °C. As the temperature further rose to 60 °C, both the modulus and ultimate strength of WPC continued to decrease, reaching only 58.7% and 58.6%, respectively, of those at 40 °C. This indicates that the WPC became more sensitive to temperature with higher temperatures.
2. At 20 °C, the stress-strain relationship of the WPC exhibited linear behavior and brittle failure. However, as the temperature increased, the material showed some ductility, and the stress-strain relationship became nonlinear, which could be predicted using the Popovics correction model under different high-temperature conditions.
3. The creep deformation of WPC was positively correlated with temperature and stress level. When the stress levels were 15% and 30%, the creep deformation increased continuously with temperature. When the stress level was 45%, the creep deformation first increased and then decreased with increasing temperature. When the temperature remained constant, the creep deformation increased with increasing stress level.
4. When the temperature remained constant, the fitting degree of the Findley model for short-term creep of WPC improved with increasing stress level. However, when the stress level was constant, the fitting effect decreased with increasing temperature. The Findley model exhibited significant distortion in fitting the creep performance of specimens tested under the condition of 60 °C and 15% stress level.
5. The fractional order model exhibited a good fit for the steady-state creep stage of WPC under various temperature conditions. The regression coefficients were significantly higher compared to the Findley model, allowing for a reliable prediction of the short-term creep performance of WPC under various operating conditions.

ACKNOWLEDGMENTS

The authors gratefully acknowledge the support by the Project of Social Sciences Foundation of Jiangsu Province of China (24YSD006), the project of production, education and research of Jiangsu Province and Science (BY2022117, BY20240764), the Project of Sentai WPC Group Co., Ltd, the Education Science Planning Project of Jiangsu Province of China (C/2023/01/33), the Project of Jiangsu Higher Education Association (2024CXJG066), and Technology Plan Project of Nanjing Construction Industry (Ks2207) for financially supporting this study.

Conflict of Interest

The authors confirm that there is no conflict of interest.

REFERENCES CITED

Alrubaie, M., Lopez-Anido, R., and Gardner, D. (2020a). "Flexural creep behavior of high-density polyethylene lumber and wood plastic composite lumber made from thermally modified wood," *Polymers* 12(02), article 262. <https://doi.org/10.3390/polym12020262>

Alrubaie, M., Lopez-Anido, R., Gardner, D., Tajvidi, M., and Han, Y. (2020b). "Modeling the hygrothermal creep behavior of wood plastic composite (WPC) lumber made from thermally modified wood," *Journal of Thermoplastic Composite Materials*, 33(08), 1109-1124. <https://doi.org/10.1177/0892705718820404>

Alrubaie, M., Lopez-Anido, R., Gardner, D., Tajvidi, M., and Han, Y. (2020c). "Experimental investigation of the hygrothermal creep strain of wood–plastic composite lumber made from thermally modified wood," *Journal of Thermoplastic Composite Materials* 33(09), 1248-1268. <https://doi.org/10.1177/0892705718820398>

Alrubaie, M., Gardner, D., and Lopez-Anido, R. (2020d). "Modeling the long-term deformation of a geodesic spherical frame structure made from wood plastic composite lumber," *Applied Sciences-Basel* 33(09), 1248-1268. <https://doi.org/10.3390/app10145017>

ASTM D143-14 (2014). "Standard test methods for small clear specimens of timber," ASTM International, West Conshohocken, PA, USA.

ASTM D3130-11 (2019). "Standard specification for n-propyl acetate (96% grade)," ASTM International, West Conshohocken, PA, USA.

Chang, F.-C., Chen, C.-Y., Wang, T.-L., Kuan, C.-S., and Wu, J.-H. (2018). "Effects of temperature-induced strain on creep behavior of wood-plastic composites," *Wood Science & Technology* 52(5), 1213-1227. <https://doi.org/10.1007/s00226-018-1033-y>

Dai, B., Huo, R., Wang, K., Z., and Fang, H. (2022). "Study on bending creep performance of GFRP-reinforced PVC-based wood-plastic composite panels," *Polymers* 14(22), article 4789. <https://doi.org/10.3390/polym14224789>

Elsheikh, A. H., Panchal, H., Shanmugan, S., Muthuramalingam, T., El-Kassas, A. M., and Ramesh, B. (2022). "Recent progresses in wood-plastic composites: Pre-processing treatments, manufacturing techniques, recyclability, and eco-friendly assessment," *Cleaner Engineering and Technology* 8, article 100450. <https://doi.org/10.1016/j.clet.2022.100450>

Feng, L., and Zhao, C.-Y. (2022). "Analysis of creep properties and factors affecting

wood plastic composites," *Polymers* 14(14), article 2814. <https://doi.org/10.3390/polym14142814>

Fu, H.-T., Dun, M.-Y., Wang, H.-G., Wang, W.-H., Ou, R.-X., Wang, Y.-G., Liu, T., and Wang, Q.-W. (2020). "Creep response of wood flour-high-density polyethylene/laminated veneer lumber coextruded composites," *Construction and Building Materials* 237, article 117499. <https://doi.org/10.1016/j.conbuildmat.2019.117499>

Golmakani, M. E., Wiczenbach, T., Malikan, M., Aliakbari, R., and Eremeyev, V. A. (2021). "Investigation of wood flour size, aspect ratios, and injection molding temperature on mechanical properties of wood flour/polyethylene composites," *Materials* 14(12), article 3406. <https://doi.org/10.3390/ma14123406>

Golmakani, M. E., Wiczenbach, T., Malikan, M., Mahoori, S. M., and Eremeyev, V. A. (2021). "Experimental and numerical investigation of tensile and flexural behavior of nanoclay wood-plastic composite," *Materials* 14(11), article 2773. <https://doi.org/10.3390/ma14112773>

Heymans, N., Bauwens, J.-C., and Bauwens-Crowet, C. (1994). "Fractal rheological models and fractional differential equations for viscoelastic behavior," *Rheologica Acta* 33, 210-219. <https://doi.org/10.1007/BF00437306>

Liu, P., Huang, Y., and Zhang, H. (2013). "Progress in research on the creep behavior of resin composites," *Glass Fiber Reinforced Plastic/Composite Materials* (3), 109-117 (in Chinese).

Pulngern, T., Chitsamran, T., Chucheepsakul, S., Rosarpitak, V., Patcharaphun, S., and Sombatsompop, N. (2016). "Effect of temperature on mechanical properties and creep responses for wood/PVC composites," *Construction and Building Materials*, 111, 191-198. <https://doi.org/10.1016/j.conbuildmat.2016.02.051>

Ratanawilai, T., and Srivabut, C. (2021). "Physico-mechanical properties and long-term creep behavior of wood-plastic composites for construction materials: Effect of water immersion times," *Case Studies in Construction Materials* 16, article e00791. <https://doi.org/10.1016/j.cscm.2021.e00791>

Van den Oever, M., and Molenveld, K. (2019). "Creep deflection of wood polymer composite profiles at demanding conditions," *Case Studies in Construction Materials* 10, article e00224. <https://doi.org/10.1016/j.cscm.2019.e00224>

Wu, Y.-F., and Wei, Y.-Y. (2015). "General stress-strain model for steel- and FRP-confined concrete," *Journal of Composites for Construction* 19(4), article 04014069. [https://doi.org/10.1061/\(ASCE\)CC.1943-5614.0000511](https://doi.org/10.1061/(ASCE)CC.1943-5614.0000511)

Xi, F., and Zhao, L.-L. (2022). "Experimental study of the compressive properties of a wood-plastic composite at different temperatures," *Polymer Composites* 43(10), 7372-7378. <https://doi.org/10.1002/pc.26815>

Xi, F., Zhao, L.-L., Wei, Y., Yi, J.-Y., and Zhao, K. (2023). "Effect of temperature on the bending and creep properties of wood plastic composites," *Polymer Composites* 44(8), 4612-4622. <https://doi.org/10.1002/pc.27425>

Zhang, G.-Q., Zhao, L.-L., Zhao, K., and Chen, L.-Y. (2024). "Short-term creep properties of WPC at different temperatures—An experimental and numerical investigation at different stress levels," *Polymer Composites* 45(12), 11480-11486. <https://doi.org/10.1002/pc.28580>

Zhao, L.-L., Xi, F., Wang, G.-Y. (2021). "Calculation model for uniaxial stress-strain relationship of wood-plastic composites," *Polymer Composites* 42(12), 6664-6671. <https://doi.org/10.1002/pc.26330>

Zhao, L.-L., Wei, Y., Zhang, G.-W., Xi, F. (2022). "Short-term creep properties and creep model of wood-plastic composites," *Polymer Composites* 43(2), 924-933. <https://doi.org/10.1002/pc.26422>

Zhao, L.-L., Li, H.-C., Wei, Y., Xi, F., and Zhao, K. (2025). "Flexural properties on aluminum alloy-wood plastic composite beam strengthened by concrete," *Construction and Building Materials* 460, article 139792. <https://doi.org/10.1016/j.conbuildmat.2024.139792>

Zong, G.-G., Hao, X.-L., Hao, J.-X., Tang, W., Fang, Y.-Q., Ou, R.-X., and Wang, Q.-W. (2020). "High-strength, lightweight, co-extruded wood flour-polyvinyl chloride/lumber composites: Effects of wood content in shell layer on mechanical properties, creep resistance, and dimensional stability," *Journal of Cleaner Production* 244, article 118860. <https://doi.org/10.1016/j.jclepro.2019.118860>

Article submitted: November 10, 2025; Peer review completed: December 20, 2025; Revised version received and accepted: December 29, 2025; Published: January 12, 2026. DOI: 10.15376/biores.21.1.1824-1835